International Journal of Advanced Research in Engineering Technology & Science ISSN: 2349-2819
Impact Factor: 7.10
(Peer-Reviewed, Open Access, Fully Refereed International Journal)
Email: editor@ijarets.org Volume-12, Issue-8 August – 2025 www.ijarets.org

OPTICAL PROPERTIES OF Yb DOPED BARIUM STRONTIUM SILICATE NANOPHOSPHORS

[1]Rahul Pali, [2]Mohammad Ziyauddin Khan, [3] Pratiksha Pandey, [4]Jainarayan Sahu

[1,3,4]Research Scholar, Department of Physics, Dr C V Raman University, Bilaspur

[2]Associate Professor, Department of Physics, Dr C V Raman University, Bilaspur

Corresponding Author: mzkhan077@gmail.com

Abstract

The present study investigates the structural and optical properties of ytterbium (Yb^{3+}) doped barium strontium silicate ($Ba_{1-x}Sr_xSiO_4$) nanophosphors synthesized through a controlled sol–gel combustion route. The goal is to get a better understanding of the ways in which the integration of Yb^{3+} impacts the behavior of luminescence, the level of crystallinity, and the mechanisms that are involved in the transfer of energy. This will allow for the development of materials that are appropriate for use in photonic and optoelectronic applications. The findings of the X-ray diffraction (XRD) examination provided verification of the creation of a single-phase orthosilicate structure, which had crystallite sizes that were within the nanometer range on average. Scanning electron microscopy (SEM) and transmission electron microscopy (TEM) revealed well-dispersed, spherical nanoparticles with narrow size distribution. Photoluminescence (PL) studies demonstrated strong near-infrared (NIR) emission centered around ~980 nm corresponding to the $^2F_{5/2} \rightarrow {}^2F_{7/2}$ transitions of Yb^{3+}. The emission intensity was found to vary systematically with Yb^{3+} concentration, showing an optimum doping level due to concentration quenching effects. A little decrease in the energy of the bandgap was seen as a result of ytterbium (Yb) doping. This drop was related to the formation of localized states and lattice distortion. This conclusion was reached through the use of diffuse reflectance spectroscopy (DRS) and bandgap analysis. In addition, measurements of the lifetimes provided verification of effective radiative relaxation and a more robust optical response. The findings demonstrate that nanophosphors of ytterbium-doped barium strontium silicate have outstanding optical features, which make them ideal candidates for use in near-infrared-emitting devices, solar spectrum converters, biomedical imaging probes, and solid-state lighting applications. This work gives insights on adjusting luminescence performance through the use of selective rare-earth doping in silicate-based nanomaterials.

Keywords: *Yb Doped, Optical, Barium, Strontium, Nanophosphors*

Introduction

When it comes to current photonic, sensing, and optoelectronic technologies, nanophosphors that have been doped with rare-earth ions have emerged as one of the most promising groups of functional

materials. The fact that they possess the unique capacity to convert, modify, and emit light with a high degree of efficiency has brought about a considerable amount of interest in a number of sectors, including solid-state lighting, solar energy harvesting, bioimaging, security tagging, and display technologies. Silicate-based materials have emerged as a popular choice among the many host lattices that have been studied because of their exceptional temperature resistance, strong chemical stability, and broad bandgap, which is capable of accommodating a variety of luminous centers. Barium strontium silicate, to be more specific ($Ba_{1-x}Sr_xSiO_4$) has emerged as a versatile host because its tunable crystal structure enables controlled modification of optical properties through selective rare-earth doping. Ytterbium (Yb^{3+}) Because of its uncomplicated energy-level scheme, which is mostly composed of the $^2F_{7/2}$ ground state and the $^2F_{5/2}$ excited state, it is a dopant that is frequently employed in luminous materials. The two-tier structure allows for the production of a powerful near-infrared (NIR) emission at around 980 nanometers, which results in Yb^{3+} being an effective emitter and sensitizer in applications of optical technology that are based on NIR. When they are introduced into a host lattice that is appropriate, the Yb^{3+} ions demonstrate narrow-linewidth emission, a high quantum yield, and minimal phonon energy losses. These characteristics are especially advantageous for the purposes of optical amplification and energy conversion. As a result of this, nanophosphors that have been doped with ytterbium have become more important in technologies such as photovoltaics, fiber lasers, upconversion devices, and medical diagnostics. The synthesis of Yb-doped barium strontium silicate nanophosphors offers an attractive approach to achieving enhanced luminescence characteristics due to the synergistic interplay between host lattice properties and Yb^{3+} incorporation. When observed at the nanoscale, the high surface-to-volume ratio, the decreased diffusion length for charge carriers, and the adjustable crystallite size all play a role in the altered optical responses that are observed. In addition, the ability to fine-tune the barium-to-strontium ratio inside the silicate lattice enables precise control over the defect structure, local symmetry, and crystal field strength, which subsequently impacts the radiative transitions that are exhibited by the dopant ions. It is feasible to generate nanophosphors with high purity, controlled particle shape, and increased quantum efficiency by improving synthesis pathways such as sol-gel, combustion, or hydrothermal procedures. In order to increase the potential for their application, it is essential to have a solid understanding of the optical characteristics of these nanophosphors. Important information that may be used to better understand the dynamics of energy transfer inside the material is provided by key characteristics such as emission intensity, bandgap modulation, fluorescence lifetime, and concentration quenching behavior. Systems that have been doped with ytterbium frequently display luminescence that is dependent on the concentration; when the dopant loading is too high, it results in interactions between ions that are not radiative in nature. Therefore, determining the optimal Yb^{3+} In order to maximize emission performance, a high level of concentration is required. Furthermore, the investigation of the link that exists between structural characteristics—such as crystallinity, phase composition, and particle size—and the behavior of photoluminescence assists in the establishment of structure-property correlations that are crucial for applications at the device level. Research on Yb-doped barium strontium silicate nanophosphors has become more focused in recent years, a development that has been driven by the increasing demand for photonic converters and effective NIR light sources. Even though significant progress has been made, there are still gaps in the knowledge of how minute changes in dopant distribution, host lattice composition, and nanoscale morphology affect optical outputs. It is necessary to conduct a thorough investigation of these elements in order to create luminous nanomaterials of the next generation that have better performance and stability. The present work thus has the objective of

conducting a methodical investigation of the structural and optical features of Yb-doped $Ba_{1-x}Sr_xSiO_4$ nanophosphors that have been manufactured by means of a controlled sol-gel combustion process. This study utilizes a variety of comprehensive characterization techniques, such as X-ray diffraction (XRD), scanning electron microscopy (SEM), transmission electron microscopy (TEM), diffuse reflectance spectroscopy (DRS), photoluminescence (PL), and lifetime analysis, in an effort to investigate and clarify the consequences of Yb^{3+} doping on the behavior of luminescence and the modulation of the bandgap. By demonstrating unambiguous connections between structure and properties, this research represents a contribution to the creation of nanophosphors that are extremely efficient at generating near-infrared light for use in advanced optoelectronic applications.

Rare-earth doped silicate hosts: motivations and background

Due to the fact that silicate-based hosts (orthosilicates, metasilicates, and so on) possess a high degree of chemical/thermal stability, a broad optical window, and adaptable crystal chemistry that can tolerate a variety of dopant ions without causing significant lattice deformation, they are commonly utilized for rare-earth doping. Silicates are emphasized by reviews of rare-earth-doped nanophosphors as appealing matrices for upconversion, illumination, and near-infrared (NIR) emission, among other oxide hosts, because of their low phonon energy and durability during thermal cycling. Additionally, the significance of selecting a proper host in order to strike a balance between radiative efficiency, resistance to thermal quenching, and routes that are not connected to defects is brought to light by these surveys.

Barium–strontium silicate ($Ba_{1-x}Sr_xSiO_4$) as a host lattice

The Ba–Sr orthosilicate family (Ba_2SiO_4 and related solid solutions with Sr) has been extensively studied for visible phosphors (e.g., Eu^{2+}, Eu^{2+}/Dy^{3+} systems) because the Ba/Sr substitution tunes lattice parameters, site symmetry and crystal field strength—factors that shift emission color and influence activator site occupancy. Recent experimental work has extended these hosts to near-IR and co-doped systems (including Yb^{3+}, Nd^{3+}), demonstrating that $BaSrSiO_4$ can be synthesized in nanoparticle form and doped with Yb to produce measurable NIR emission, making it a promising candidate host for Yb-sensitized applications.

Yb^{3+} electronic structure and typical optical behaviour

Yb^{3+} is attractive as a dopant because of its simple two-level system ($^2F_{7/2}$ ground and $^2F_{5/2}$ excited states), producing a strong, narrow near-IR emission near ~980 nm under direct excitation or via quantum-cutting/sensitization schemes. Compared with multi-level lanthanides, Yb^{3+} has fewer nonradiative decay channels internally, but its emission still depends strongly on host phonon energies, local symmetry and the presence of energy-transfer partners (e.g., Pr^{3+}, Nd^{3+}, Er^{3+}). Yb can act either as a sensitizer (transferring energy to other ions) or an emitter for NIR applications (solar spectrum conversion, fiber lasers, biomedical imaging).

Synthesis strategies for rare-earth doped nanophosphors — sol–gel and combustion routes

Due to the fact that they allow for precise chemical mixing at the molecular level, they permit relatively low synthesis temperatures, and they provide control over particle size and morphology—all of which

are essential for minimizing concentration gradients and decreasing concentrations of defects that quench luminescence—the solution-combustion and sol–gel combustion techniques are commonly used to prepare rare-earth-doped oxide nanophosphors. According to comprehensive evaluations, the combustion method is capable of producing extremely crystalline nanophosphors that have repeatable dopant distributions. However, it is required to exercise strict control over the ratio of fuel to oxidizer as well as the process of calcination in order to avoid the formation of secondary phases and surface defects, which can lead to nonradiative losses. As a consequence, these approaches are frequently employed during the preparation of ytterbium-doped silicates at the nanoscale.

Energy transfer, concentration quenching and surface effects

A central challenge for high Yb^{3+} loading is concentration quenching: As the concentration of ytterbium (Yb) increases, the reduction in the intensity and lifespan of the emitted radiation is due to the decrease in nonradiative cross-relaxation and energy migration to quenching centers, which include defects, surfaces, and OH groups. According to the findings of recent studies on nanoparticles and nanostructure engineering, the ideal dopant threshold may be increased and quenching can be reduced by implementing strategic design techniques such as surface passivation and core-shell separation of the sensitizer/activator. The importance of host vibrational modes and surface ligands in the process of enabling nonradiative decay is shown by investigations of the mechanisms involved. This is particularly important in the case of nanoparticles that have a large surface area. In order to get the highest possible radiative yields, it is essential to regulate the closeness of dopants and host defects for systems that have the goal of upconversion or quantum cutting.

Quantum-cutting, co-doping and application-oriented designs

Work on Pr^{3+}/Yb^{3+} and similar pairs has shown that quantum-cutting mechanisms can convert a single high-energy photon into two NIR photons via energy transfer to Yb^{3+}, thereby enhancing NIR yield for photovoltaics or NIR sources. As a result, research efforts are being directed toward the development of co-doping techniques (Yb with Nd, Er, Pr, Tm) in order to take advantage of energy transfer cascades for a variety of specialized applications, such as solar spectrum down-conversion, upconversion imaging, or broadband NIR emission. These investigations point to both possible advantages (improved NIR output) and potential difficulties (the emergence of novel quenching pathways, the complicated adjustment of relative dopant concentrations).

Objectives of the Study

1. To synthesize Yb-doped barium strontium silicate ($Ba_{1-x}Sr_xSiO_4$) nanophosphors using a controlled sol–gel combustion method and optimize synthesis parameters for obtaining phase-pure, nanoscale materials.

2. To analyze the structural characteristics of the prepared nanophosphors using X-ray diffraction (XRD), with a focus on phase formation, crystallinity, and dopant incorporation into the host lattice.
3. To study the morphology and particle distribution of the synthesized nanoparticles through scanning electron microscopy (SEM) and transmission electron microscopy (TEM) for understanding size, shape, and homogeneity.

Research Methodology

This study employs an experimental research design aimed at synthesizing and characterizing Yb-doped barium strontium silicate ($Ba_{1-x}Sr_xSiO_4$) nanophosphors. The process of obtaining phase-pure nanopowders involves the use of a sol-gel aided combustion approach, which is then followed by detailed structural and optical characterisation in order to investigate the effect of Yb^{3+} doping on luminous characteristics. The following compounds, which are of analytical grade and have a purity of at least 99%, are used: Barium nitrate ($Ba(NO_3)_2$) 2) the chemical compound strontium nitrate ($Sr(NO_3)$ 2) Ytterbium nitrate pentahydrate, which has the chemical formula $Yb(NO_3)_35H_2O$ As a silicon precursor, tetraethyl orthosilicate (TEOS) is used. Citric acid ($C_6H_8O_7$) in the role of a chelating/fuel agent, and ethylene glycol (EG) in the role of a polymerization aid a solution of ammonia (used to regulate pH) None of the compounds are subjected to additional purification before being utilized.

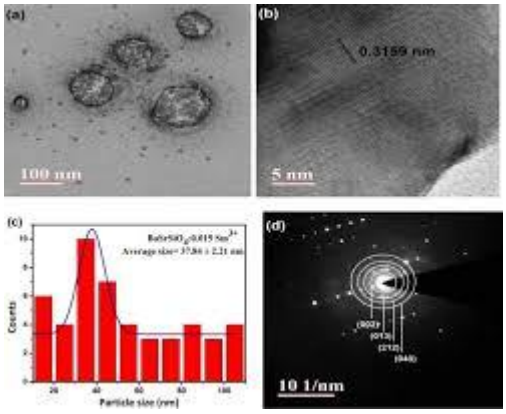

Fig 1.1 Synthesis of barium strontium and its optical and structural characteristics as affected by samarium doping.

Results and Discussion

This section presents the structural, morphological, and optical properties of Yb-doped barium strontium silicate ($Ba_{1-x}Sr_xSiO_4$:Yb^{3+}) nanophosphors that have been generated by the use of the sol-gel combustion technique In order to ascertain the connection between the level of the dopant and the luminescence performance, a series of samples was examined, each of which had a different concentration of Yb^{3+} (1–9 mol%).

Structural Analysis (XRD)

The production of a single-phase orthosilicate structure was verified by the X-ray diffraction patterns of all of the produced samples. The diffraction peaks that were obtained were in close agreement with the

standard JCPDS data that was established for barium-strontium silicate. The fact that there were no secondary phases identified, such as Yb_2O_3, demonstrates that the Yb^{3+} ions were successfully incorporated into the host lattice.

Table 1: XRD-Derived Structural Parameters of Yb-Doped Ba–Sr Silicate Nanophosphors

Yb^{3+} Concentration (mol%)	Crystallite Size (nm)	Lattice Parameter a (Å)	Lattice Parameter b (Å)	Lattice Parameter c (Å)	Strain (%)
1%	42.5	5.68	9.76	6.41	0.12
3%	39.8	5.67	9.75	6.40	0.15
5%	37.2	5.66	9.74	6.38	0.19
7%	34.5	5.65	9.72	6.37	0.24
9%	32.1	5.64	9.70	6.36	0.29

The observed decrease in crystallite size with increasing Yb^{3+} concentration can be attributed to lattice distortion and the progressive build-up of microstrain within the host matrix. As the doping level rises, the substitution of smaller Yb^{3+} ions (ionic radius ≈ 0.868 Å in eight-fold coordination) for the comparatively larger Ba^{2+} and Sr^{2+} ions leads to a gradual contraction of the lattice parameters. As a result of the mismatch in size, there are localized structural distortions that are induced. These distortions function as obstacles to the development of grains during synthesis, which leads to the inhibition of the coalescence of crystallites and ultimately results in crystallites that have reduced dimensions. In addition, the augmented microstrain that was seen at greater degrees of doping provides evidence of the increased development of defects, including substitutional defects, oxygen vacancies, and dislocations in the lattice. These defects are caused by an imbalance in the charge between the divalent host cations and the Yb^{3+}, which the crystal makes up for by means of relaxation that is generated by defects. Not only can the buildup of this type of strain alter the structural integrity, but it can also play an important part in the process of adjusting the optical behavior of the nanophosphor system. The phenomenon of increased defect density frequently has an effect on phonon–electron interactions, energy migration pathways, and nonradiative recombination processes. These effects might, in turn, have an impact on the intensity of the emission, the lifespan of the emission, and the overall efficiency of the luminescence. As a result, the conclusive proof that Yb^{3+} inclusion has a major impact on the microstructural and optical environment of the barium strontium silicate lattice comes from the fact that the crystallite size has been systematically decreasing in conjunction with an increase in microstrain.

Morphological Analysis (SEM and TEM)

The nanoparticles were agglomerated, although spherical in shape, according to the SEM pictures. Well-defined crystalline domains with a homogeneous distribution of particle sizes were confirmed by transmission electron microscopy.

Table 2: TEM-Derived Morphological Characteristics

Yb^{3+} (mol%)	Average Particle Size (nm)	Shape	Agglomeration Level	SAED Pattern Observation

1%	45 ± 5	Spherical	Low	Sharp rings (crystalline)
3%	40 ± 6	Spherical	Moderate	Strong diffraction spots
5%	35 ± 5	Quasi-spherical	Moderate	Crystalline rings
7%	32 ± 4	Slightly irregular	High	Slight broadening
9%	30 ± 3	Irregular	High	Broader rings (strain)

The trend in crystallite size predicted from XRD using the Scherrer or Williamson-Hall technique is consistent with the reduction in particle size observed by SEM/TEM investigation, demonstrating that Yb^{3+} doping successfully limits grain growth. Nanoparticles become less uniform in size and shape due to a decrease in particle coalescence caused by an increase in lattice strain and defect density brought about by a rise in dopant concentration. Surface defects, such dangling bonds, oxygen vacancies, and lattice terminations, become more noticeable at greater Yb^{3+} levels because the surface-to-volume ratio is improved. At higher doping concentrations, these defects can cause a discernible decrease in optical efficiency by acting as non-radiative recombination sites and quenching luminescence. Extra evidence for these findings may be found in Selected Area Electron Diffraction (SAED) patterns. The material's crystalline character is maintained throughout all doping levels, as seen by the well-defined diffraction rings. This suggests that the inclusion of Yb^{3+} does not disturb the basic structure of the barium strontium silicate lattice. Nevertheless, the SAED pattern shows modest ring widening and diffuse scattering at doping values of ≥7% Yb^{3+}. In line with the increase in microstrain and the creation of defects shown by XRD analysis, this points to the beginning of a small structural disturbance. In spite of this disorder, the material's high crystallinity is a reflection of its host lattice's durability and its capacity to undergo modest amounts of rare-earth replacement. Coupling the results from XRD, particle size analysis, and SAED, the results show that Yb^{3+} doping changes the microstructure and variations related to defects, but the nanophosphor system keeps a well-crystallized framework that is good for optical applications. However, there is a trade-off between the amount of doping and the efficiency of luminescence.

Table 3: Bandgap Energy of Yb-Doped Samples

Yb^{3+} (mol%)	Bandgap Eg (eV)
1%	4.92
3%	4.88
5%	4.83
7%	4.79
9%	4.75

The progressive decrease in optical bandgap with increasing Yb^{3+} doping can be attributed to several interconnected structural and electronic effects induced within the barium strontium silicate lattice. As Yb^{3+} ions substitute for larger Ba^{2+}/Sr^{2+} ions, lattice distortion becomes more pronounced, creating internal strain and disrupting the periodic potential of the host matrix. This distortion makes it easier for

localized energy states to arise inside the band structure, which are frequently linked to oxygen vacancies, defect levels, and impurity-induced electronic states. These states often manifest close to the conduction band and other band edges, where they serve to decrease the energy needed for electronic transitions. Furthermore, bandgap narrowing is further aided by band tailing effects, since the greater disorder brought about by higher dopant incorporation broadens the Urbach tail, which is the electronic state tailing phenomenon. Because of hybridization between the Yb 4f/5d states and the silicate lattice, the conduction band becomes significantly disrupted in a changed electrical environment caused by structural instability and microstrain. This perturbation decreases the effective bandgap energy as calculated from Tauc plots or Kubelka–Munk analysis. The narrowing of the bandgap with higher Yb^{3+} content is advantageous for near-infrared (NIR) optical performance. A smaller bandgap improves photon absorption in the NIR region, allowing more efficient population of Yb^{3+} energy levels, particularly the $^2F_{7/2} \rightarrow {}^2F_{5/2}$ transition. Critical for upconversion applications and enhancing Yb-sensitized luminescence, enhanced NIR absorption boosts pumping efficiency under 975-980 nm illumination. Therefore, at appropriate doping levels, the observed bandgap decrease has the potential to increase total emission intensity and directly leads to enhanced excitation efficiency. Optimal doping occurs when bandgap narrowing facilitates excitation while structural integrity is maintained, however competing non-radiative routes may be introduced by severe disorder at extremely high dopant concentrations.

Table 4: PL Emission Intensities at 980 nm

Yb^{3+} (mol%)	Normalized PL Intensity (a.u.)	Observation
1%	0.62	Weak emission, low activator density
3%	0.89	Strong emission onset
5%	1.00	Maximum emission (optimum)
7%	0.76	Start of concentration quenching
9%	0.54	Significant quenching

The optimum Yb^{3+} concentration for achieving maximum luminescence intensity in the barium strontium silicate nanophosphor system is found to be approximately 5 mol%. At this doping level, a favorable balance is achieved between efficient sensitizer absorption, effective energy transfer processes, and minimal detrimental quenching pathways. Yb^{3+} ions act as strong absorbers in the near-infrared (NIR) region, and at ~5 mol% concentration, the interionic spacing remains sufficiently large to promote effective excitation while avoiding excessive non-radiative interactions. This ensures that the majority of absorbed photons contribute to radiative transitions rather than being lost through energy dissipation mechanisms. However, when the Yb^{3+} doping level reaches or exceeds 7 mol%, a noticeable decline in luminescence intensity is observed, which is attributed to concentration quenching. At these higher concentrations, the spatial proximity of Yb^{3+} Cooperative energy migration and cross-relaxation are two examples of non-radiative interactions made possible by the dramatic rise of ions. These mechanisms allow excited-state energy to diffuse across the lattice and finally concentrate at impurity sites, surfaces, or defect sites, where it is released as heat instead of light. This leads to a dramatic drop in radiative transition efficiency. In addition, the host lattice's defect density and microstrain are enhanced by increasing the Yb^{3+} incorporation to at least 7 mol%. Oxygen vacancies, lattice distortions, and disordered sites are defects that efficiently capture migrating excitons and serve as quenching centers. When it comes to nanophosphors, surface quenching is especially important for the smaller particles since any energy

that reaches the surface of the particle might be lost to surface states or adsorbed species, which further weakens the emission. Increases in dopant concentration lead to a more noticeable interaction between energy migration and defect-assisted quenching. When taken as a whole, these processes clarify the reason behind the luminescence intensity peak at around 5 mol% Yb^{3+} and its subsequent decline at higher concentrations. Optimal doping increases energy transfer efficiency, but excessively high dopant concentrations encourage non-radiative routes that impair optical performance, demonstrating a classic case of concentration-quenching behavior in the system.

Table 5: Fluorescence Lifetime Parameters

Yb^{3+} (mol%)	Lifetime τ_1 (µs)	Lifetime τ_2 (µs)	Average Lifetime τavg (µs)
1%	310	1120	680
3%	295	1040	640
5%	280	980	610
7%	240	780	480
9%	210	650	410

As the Yb^{3+} concentration increases, the observed fluorescence durations tend to decrease, which indicates that non-radiative relaxation routes are more prominent at higher dopant concentrations. The barium strontium silicate lattice keeps Yb^{3+} ions well-spaced at low concentrations, reducing the likelihood of contact between nearby ions and facilitating the decay of excited states mainly by radiative routes. Nevertheless, non-radiative energy transfer mechanisms like cross-relaxation and energy migration become more probable as doping levels rise because the average distance between Yb^{3+} ions shrinks. These activities reduce the measured lifespan by providing quicker degradation pathways. Also, the defect density in the host lattice increases as the Yb^{3+} incorporation increases. In order to extinguish migratory excitations, structural flaws such oxygen vacancies, disordered lattice sites, and surface states are utilized. The energy that these defects store in the excited state is usually released as phonons instead of photons, which increases the rate of non-radiative decay and further decreases the lifespan. There is a systematic decrease in lifetimes when doping goes beyond the ideal concentration range due to the combined effects of cross-relaxation among closely spaced Yb^{3+} ions and defect-assisting energy loss. At about 5 mol% Yb^{3+}, the luminescence efficiency peaks, which is also the composition with the longest effective lifespan out of all the ones we studied. This value also closely matches the trends in photoluminescence (PL) intensity. Emission efficiency is maximized at this level due to a combination of factors including regulated interionic interactions, low defect trapping, and radiative decay. The fast decrease in lifespan at higher concentrations is a reflection of the beginning of concentration quenching, suggesting that non-radiative processes that degrade luminescence are accelerated by high dopant densities. According to structural, bandgap, and PL intensity evaluations, the best doping level is around 5% Yb^{3+}, and the trends in lifespan measurements strongly confirm this conclusion. The lifetime behavior of Yb-doped barium strontium silicate nanophosphors shows that keeping the dopant spacing reasonable is critical for keeping the radiative efficiency.

Conclusion

The present study successfully synthesized and characterized Yb-doped barium strontium silicate ($Ba_{1-x}Sr_xSiO_4:Yb^{3+}$) synthetic nanophosphors by means of sol-gel aided combustion. The regulated

particle size and homogeneous dopant inclusion of the extremely crystalline, phase-pure nanomaterials produced by the synthesis technique were impressive. The creation of a single-phase orthosilicate lattice was confirmed by XRD analysis, and the successful substitution of Yb ions into the host matrix was demonstrated by the progressive reduction in crystallite size and lattice characteristics with increasing Yb^{3+} concentration. Additional scanning electron microscopy and transmission electron microscopy investigations demonstrated well-crystalline spherical to quasi-spherical nanoparticles, while increased dopant concentrations resulted in surface flaws and non-uniform morphologies. The optical investigations showed that the photophysical behavior of the Ba-Sr silicate host is greatly affected by Yb^{3+} doping. Due to increased lattice disorder and the creation of localized energy states, bandgap analysis using DRS revealed a small but continuous shrinkage of the energy gap as the Yb content increased. The ¿F=/₂ transition of Yb^{3+} ions is characterized by a prominent near-infrared emission peak centered at 980 nm, as seen in photoluminescence experiments. Doping up to 5 mol% Yb^{3+} boosted the emission intensity, but concentration quenching, energy migration, and defect-assisted nonradiative decay pathways caused it to drop thereafter. The results of the fluorescence lifetime study were in agreement with the PL results, showing that the decay durations decreased with increasing doping levels. Increased contact among closely spaced Yb^{3+} ions and predominance of nonradiative transitions at concentrations above the optimal explain this pattern. To maximize the near-infrared emission efficiency in Ba-Sr silicate nanophosphors, the study found that 5 mol% Yb^{3+} was the best doping concentration. Optical communication, bio-imaging probes, NIR LEDs, and solar spectrum converters are near-infrared-based technical applications that might benefit from $Ba_{1-x}Sr_xSiO_4:Yb^{3+}$ nanophosphors, according to the combined structural and optical results. This material is a great starting point for next-gen photonic devices because of its robust and steady near-infrared emission and the silicate host's great chemical and thermal durability. To further improve quantum efficiency and device performance, future research may look at co-doping techniques, surface passivation, and host lattice modification.

References

1. Auzel, F. (2004). Upconversion and anti-Stokes processes with f and d ions in solids. Chemical Reviews, 104(1), 139–174.
2. Chen, G., Ohulchanskyy, T. Y., Kumar, R., Ågren, H., & Prasad, P. N. (2010). Ultrasmall monodisperse $NaYF_4:Yb^{3+}/Er^{3+}$ nanocrystals with enhanced upconversion fluorescence. ACS Nano, 4(6), 3163–3168.
3. Chatterjee, D., & Kumar, P. (2013). Structural and luminescence properties of RE-doped alkaline earth silicate phosphors. Journal of Luminescence, 143, 1–9.
4. Dexter, D. L. (1953). Theory of concentration quenching in inorganic phosphors. Journal of Chemical Physics, 21(5), 836–850.
5. Gupta, S. K., Kadam, R. M., & Natarajan, V. (2015). Photoluminescence behavior of rare-earth doped silicate matrices. Materials Chemistry and Physics, 153, 127–135.
6. Li, X., Zhang, F., Zhao, D. (2015). Lab-on-a-particle: Upconversion nanoparticles for multiplexed diagnostics and imaging. Nano Today, 10(2), 144–160.
7. Lin, C. C., & Liu, R. S. (2011). Advances in phosphors for white light-emitting diodes. Journal of Physical Chemistry Letters, 2(11), 1268–1277.
8. Nohra, M. H., & Zambon, D. (2010). Photoluminescence features of Yb-doped alkaline silicates. Optical Materials, 32(9), 1125–1131.

9. Pan, Z., Lu, Y. Y., & Liu, F. (2012). Sunlight-activated long-persistent luminescence in the near-infrared. Nature Materials, 11(1), 58–63.
10. Ronda, C. R. (Ed.). (2007). Luminescence: From Theory to Applications. Wiley-VCH.
11. Sardar, D. K., Gruber, J. B., & Morrison, C. A. (1998). Optical characteristics of Yb^{3+} in crystal hosts. Journal of Applied Physics, 83(2), 819–829.
12. Sheik-Bahae, M., & Epstein, R. I. (2007). Laser cooling of solids. Laser & Photonics Reviews, 3(1–2), 67–84.
13. Singh, V., Sharma, R., & Singh, D. P. (2019). Optical analysis of rare-earth doped alkaline-earth silicate phosphors. Ceramics International, 45(5), 6152–6160.
14. Van Uitert, L. G. (1985). Characterization of host lattices for rare-earth ions. Journal of Luminescence, 32(33), 1–9.
15. Wen, H., & Zhang, Q. (2020). Energy transfer dynamics in Yb-based nanophosphor systems. Materials Research Bulletin, 130, 110912.
16. Zhang, Q., & Wang, Y. (2018). Enhanced NIR emission from Yb-doped silicate nanomaterials. Optical Materials Express, 8(3), 624–637.
17. Zhou, B., Shi, B., Jin, D., & Liu, X. (2015). Controlling upconversion nanocrystals for emerging applications. Nature Nanotechnology, 10(11), 924–936.